Optimization Study of Eggshell Extract as Inhibitor of Mild Steel Corrosion in a 30 wt% NaCl Solution

O. Oyewole[1,2], J. B. Adeoye[2]*, M. Lucas[1,2] and W. Olugbemi[1,3]

[1]*SGD9: Industry, Innovation and Infrastructure*
[2]*Department of Chemical Engineering, College of Engineering, Landmark University, Omu- Aran, Kwara State, Nigeria*
[3]*Chemical Engineering Department, Abubakar University, Zaria, Nigeria*
*Corresponding author: adeoye.john@lmu.edu.ng

Received 21/09/2022; accepted 27/12/2022
https://doi.org/10.4152/pea.2024420204

Abstract
Corrosion is a major challenge faced in industries, which has to be addressed by using inhibitors. The aim of this study was to investigate ESE as CI of MS in a 30 wt% NaCl solution. ESE was subjected to Pc analysis, to identify the presence of active ingredients that would create a good CI. CI of ESE at different C was investigated using WL, PDP, SEM, FTIR and EDXS techniques, to characterize MS samples. The best process level from the experimental design was observed at T of 24.4 ºC, IT of 6 days and ESE C of 0.4 g/L, with IE(%) of 95.5%. The presence of metabolites in ESE was confirmed by Pc analysis, which suggested the extract was a good CI. Results from PDP and WL techniques were in good agreement. SEM, FTIR and EDS data revealed that the optimal procedure level produced a stronger protective film on the MS surface. It was concluded that ESE acted as a good and environmentally friendly CI.

***Keywords*:** CR; EDXS; FTIR; IE(%); optimization; PDP; SEM; WL.

Introduction•

The increase in corrosion costs has brought about major financial problems to oil, refinery and petroleum industries, which has fostered research for CI that are also eco-friendly [1]. Corrosion is the spontaneous oxidation of most metals. It causes metals and alloys deterioration or destruction by chemical or electrochemical means [2]. Acids and chlorides are among the main sources of MS corrosion, which is a major concern in academia and industry. Furthermore, in industries like gas production and offshore oil, seawater environments are frequently used. While corrosion is most commonly associated with metals, it affects all kinds of materials. MS is a popular structural material in sugar, petrochemical, brewery, agricultural, paper, textile and marine industries, for making reaction vessels, pipes and tanks [3], since it is cheap and has usable properties. It has a carbon content of up to 0.25%, among other elements, which allows its use in several

• The abbreviations and symbols definition lists are in page 134.

products, such as structural beams, automobile bodies, kitchen appliances and cans treatment [4]. The only concern for MS is its low resistance against corrosion, particularly in acidic/saline environments. Over the years, efforts have been made to develop effective organic CI in various corrosive conditions, which generally have O, N and S heteroatoms that have higher basicity and electron density. The active centres for the adsorption process onto the metal surface are O, N, P and S. IE(%) is commonly measured in the following order: O < N < S < P [5]. Researchers are still searching for the best and most cost-effective CI. Most natural-based CI are environmentally safe chemicals that can be discarded [6]. Various plant extracts/animal wastes are able to reduce corrosion with promising efficacy. Some of them are: *Mangifera indica* [7, 25]; *Eucalyptus* LE [8]; *Mangifera ficus tikoua* LE [9]; *Saraca ashoka* aqueous seed [10]; *Tinospora crispa* extract [11]; *Bitter kola* leaf [12]; *Gentiana olivieri* extracts [13]; calcinated ES [14]; *Mango* extract [15]; *Luffa cylindrica* LE [16]; *Dioscorea septemloba* [17]; *Pterocarpus santalinoides* LE [18]; Pomegranate peel plant extracts [19]; *Paederia Foetida* LE [20]; *Katemfe* LE [21]; CNE [22]; *Corchorus Olitorus* LE [23]; and *Ficus extrasperata* extract [24].

This research was tailored to use ES for preventing corrosion, because it is a readily available and eco-friendly waste. The goal of the study was to optimize ESE as CI on MS in a 30 wt% NaCl solution.

Materials and methods

MS preparation

MS employed in this experiment came from the mechanical workshop at Landmark University in Omu-Aran, Kwara State, Nigeria. MS dimensions were 2.2 by 1.9 cm, thickness of 0.2 cm, with a 0.1 cm hole drilled in the middle. After being rinsed with distilled water and degreased with acetone, for removing any oil contaminants, MS was cleaned with emery paper, in order to expose the shiny surface, and then placed in a desiccator.

ESE preparation

ES were provided by Landmark University Pastries and dried for three days. Then, they were crushed and stored for extraction. In each procedure, 35 g ES powder were placed in a Soxhlet extractor with 300 mL ethanol, for 3 h. The solution was then concentrated and used to make the C of ESE in 30 wt% NaCl.

Corrosive medium preparation

The corrosive medium was prepared by adding 300 g NaCl to 1000 mL distilled water.

WL method

A beaker containing the prepared solution in a thermostatic water bath was used to evaluate WL for all the experimental runs predicted by BB design. T ranges used in this study were from 24.1 to 30.6 ºC, in a thermostatic water bath. This range was determined based on a 10-year survey conducted by [24], which revealed that T of seawater in Nigeria fluctuates from 24.1 to 30.6 ºC (https://www.seawatertemperature.com). C of ESE was from 0.4 to 0.8 g/L, and

IT was 3-15 days. MS coupons were weighed before and after immersion, using software-generated variations in IT, T and C of ESE, for each run.
Eq. (1) was used to compute WL of MS.

$$\Delta W = W_b - W_a \quad (1)$$

where MS weight before and after immersion in 30 wt% NaCl is W_b and W_a, respectively.
CR was calculated using eq. (2).

$$CR = \frac{\Delta W}{At} \quad (2)$$

where ΔW is MS coupon WL without and with ESE, t is IT and A is the alloy area.
IE(%) was calculated using eq. (3).

$$IE\% = \frac{Wb - Wa}{Wb} \times 100 \quad (3)$$

Pc analysis

ES were subjected to Pc analysis, in order to identify the presence of some active ingredients that would create a good CI.

Experimental design

Three variables (T, IT and C of ESE) generated 17 experimental runs by BB design. Table 1 shows the experimental ranges (low and high). Table 2 depicted the experimental design variables interactions.

Table 1: Experimental ranges (low and high).

Name and symbol	Units	Low	High
T = A	°C	24.4	30.6
IT = B	Days	3	15
Amount = C	(g/L)	0.3	0.8

Table 2: Variables interactions for 17 experimental runs.

Run	T (°C)	IT (days)	C of ESE (g/L)
1	27.5	9	0.6
2	24.4	15	0.6
3	30.6	15	0.6
4	24.4	6	0.4
5	27.5	15	0.8
6	27.5	9	0.6
7	24.4	9	0.8
8	30.6	9	0.8
9	24.4	3	0.6
10	27.5	15	0.4
11	27.5	3	0.4
12	27.5	9	0.6
13	27.5	9	0.6
14	30.6	3	0.6
15	27.5	3	0.8
16	27.5	9	0.6
17	30.6	9	0.4

Surface characterization

FTIR

FTIR analysis was used to assess MS in a 30 wt% NaCl solution: without ESE; with ESE, at its highest IE(%) (as determined by the experimental design); and via optimal process levels (validated).

SEM

SEM technique was employed to study MS morphology and best process variables in a 30 wt% NaCl solution: without ESE; with ESE at the highest IE(%) (as determined by the experimental design); and via optimal process levels (validated).

EDS

EDS revealed MS elemental components in a 30 wt% NaCl solution: without ESE; with ESE, at its highest IE(%) (as determined by the experimental design); and via optimal process levels (validated).

Electrochemical techniques

PDP study

A potentiostat was used to measure PDP plots for MS specimens in 30 wt% NaCl with various C of ESE. A magnetic stirrer was used to keep the test solution at a constant T of 24.4 ºC. After being polished, the samples were degreased with acetone, and rinsed. E_{corr} extrapolation to the linear component gave I_{corr}. Steady-state OCP was accomplished by determining the electrochemical system unchanged at the IT end. Furthermore, to obtain PDP data, the V was from -250 to +250 mV, at a SR of 1 mV/s.

Results and discussion

Discussion of Pc analysis results

ESE is a powerful CI, since it contains proteins, which are a type of amino acid, which backed up findings from [22, 25]. Pc analysis results are shown in Table 3.

Table 3: Results of Pc analysis.

Components	Percentage
N	0.93%
Protein	5.79%
Fat	1.5%
Moisture	0.5%
Ash	90%

Results of WL measurements

Tables 4-6 show the results of experiments generated with BB design. The best process level was observed in experimental run 4 with: IT of 9 days; T of 24.4 ºC, C of ESE at 0.4 g/L; and IE(%) of 95.65%. Furthermore, lowest CR was also found in experiment run 4.

Table 4: Results from the experimental runs with WL response.

Run	T (ºC)	IT (days)	C of ESE (g/L)	WL (g)
1	27.5	9	0.6	0.004
2	24.4	15	0.6	0.013
3	30.6	15	0.6	0.009
4	24.4	6	0.4	0.002
5	27.5	15	0.8	0.005
6	27.5	9	0.6	0.004
7	24.4	9	0.8	0.013
8	30.6	9	0.8	0.007
9	24.4	3	0.6	0.005
10	27.5	15	0.4	0.006
11	27.5	3	0.4	0.01
12	27.5	9	0.6	0.004
13	27.5	9	0.6	0.004
14	30.6	3	0.6	0.004
15	27.5	3	0.8	0.005
16	27.5	9	0.6	0.004
17	30.6	9	0.4	0.008

Table 5: Results from the experimental runs with CR response.

Run	T (ºC)	IT (days)	C of ESE (g/L)	CR $g/cm^2/days$
1	27.5	9	0.6	0.0015873
2	24.4	15	0.6	0.0003095
3	30.6	15	0.6	0.0002142
4	24.4	6	0.4	3.3333E05
5	27.5	15	0.8	0.0001190
6	27.5	9	0.6	0.0015873
7	24.4	9	0.8	0.0001444
8	30.6	9	0.8	0.0002777
9	24.4	3	0.6	0.0001666
10	27.5	15	0.4	0.0001428
11	27.5	3	0.4	0.0011904
12	27.5	9	0.6	0.0015873
13	27.5	9	0.6	0.0015873
14	30.6	3	0.6	0.0047619
15	27.5	3	0.8	0.0005952
16	27.5	9	0.6	0.0015873
17	30.6	9	0.4	0.0003174

Table 6: Results from the experimental runs with θ and IE response.

Run	T (ºC)	IT (days)	C of ESE (g/L)	θ	IE (%)
1	27.5	9	0.6	0.333	33.3
2	24.4	15	0.6	0.200	20
3	30.6	15	0.6	0.573	57.333
4	24.4	6	0.4	0.953	95.333
5	27.5	15	0.8	0.667	66.66677
6	27.5	9	0.6	0.333	33.3
7	24.4	9	0.8	0.560	56
8	30.6	9	0.8	0.633	63.333
9	24.4	3	0.6	0.573	57.333
10	27.5	15	0.4	0.666	66.667
11	27.5	3	0.4	0.713	71.333
12	27.5	9	0.6	0.333	33.3
13	27.5	9	0.6	0.333	33.3
14	30.6	3	0.6	0.573	57.333
15	27.5	3	0.8	0.132	13.2
16	27.5	9	0.6	0.333	33.3
17	30.6	9	0.4	0.466	46.6777

The graph for IE(%) of ESE *vs*. WL of MS is shown in Fig. 1.

Figure 1: Graph for IE(%) of ESE vs. WL of MS.

Fig. 2 shows graph of ESE IE(%) *vs*. CR of MS.

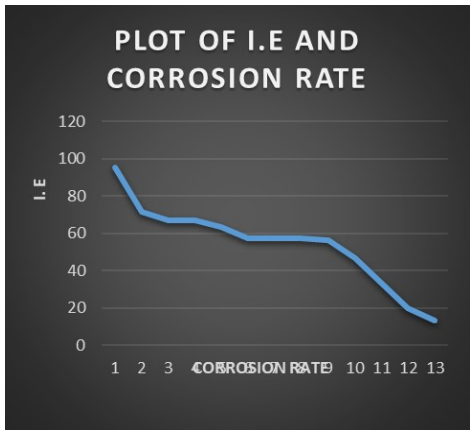

Figure 2: Graph for IE(%) of ESE vs. CR of MS.

Statistical analysis on CI of MS in 30 wt% NaCl by ESE

As shown in Table 7, the observed model F-value was 118.45.

Table 7: ANOVA.

Source	Sum of squares	DF	Square	Value	Prob > F
Model	6946.19	9	771.80	118.45 < 0.0001	significant
A	447.46	1	447.46	68.67 < 0.0001	
B	433.57		1433.57	66.54 < 0.0001	
C	683.87	1	683.87	104.96 < 0.0001	
A^2	2754.28	1	2754.28	422.71 < 0.0001	
B^2	1119.02	1	1119.02	171.74 < 0.0001	
C^2	1110.05	1	1110.05	170.37 < 0.0001	
AB	*1685.98*	1	*1685.98*	*258.76 < 0.0001*	
AC	66.10	1	66.10	10.14 < 0.0154	
BC	2760.49	1	2760.49	423.67 < 0.0001	
Residual	45.61	7	6.52		
Lack of fit	45.60	1	45.60	34201.50 < 0.0001	significant
Pure error	8.000	6	1.333		
Cor. total	6991.80		16		
Squared R	0.9935				
Pred. squared R	0.9851				
Adj. squared R	0.9844				

Model terms are significant if the "Prob > F" value is less than 0.0500. The significant model terms are: A, B, C, A^2, B2, C^2, AB, AC and BC. R^2 value of 0.9935 showed that the existing model predicted more than 99% response variability. Predicted (0.9851) and adjusted R^2 (0.9844) were found to be in good agreement. The regression eq, observed in terms of coded and actual factors, is below:

Response 1 = +33.61+9.46A-11.64B+11.69C+35.33 A^2+18.42B^2-22.43C^2
-29.40AB-4.06AC+38.96 BC (4)

where A is T, B is IT and C is ESE content.

Discussion on the 3D surface plots

Figs. 3-8 shows 3D plots for the variables interactions. They confirm the results from [27]

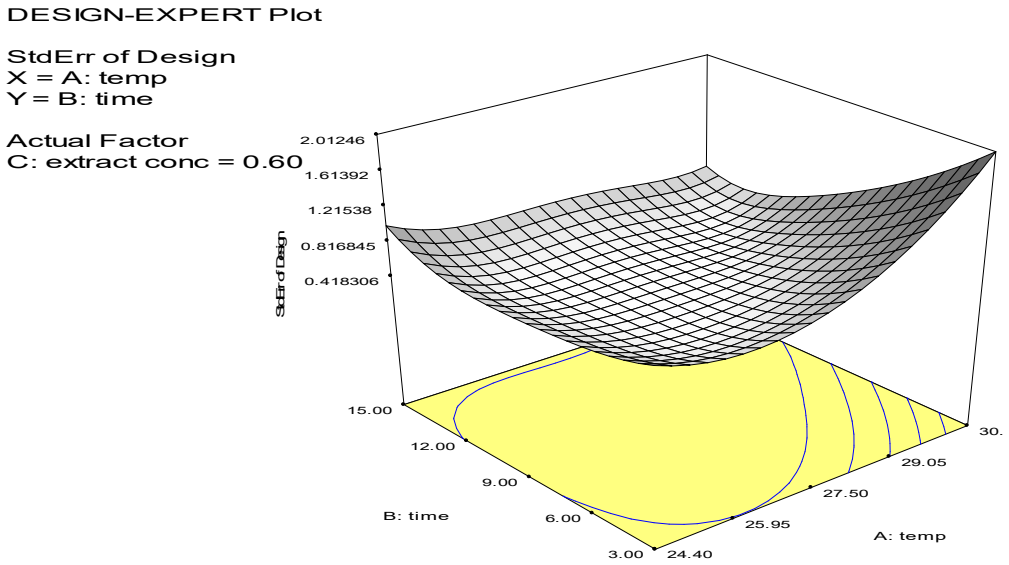

Figure 3: Plot of IT *vs.*T on C of ESE.

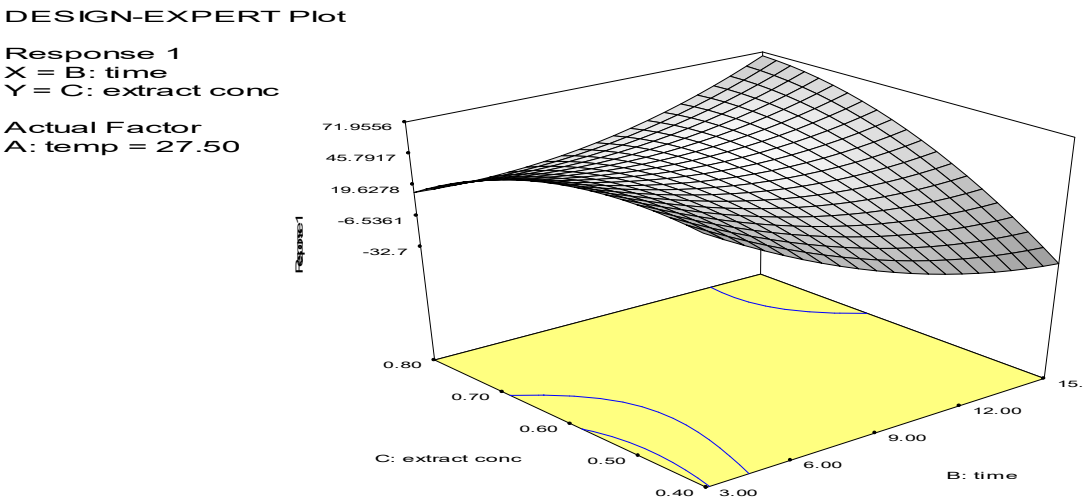

Figure 4: Plot of IT *vs.* C of ESE.

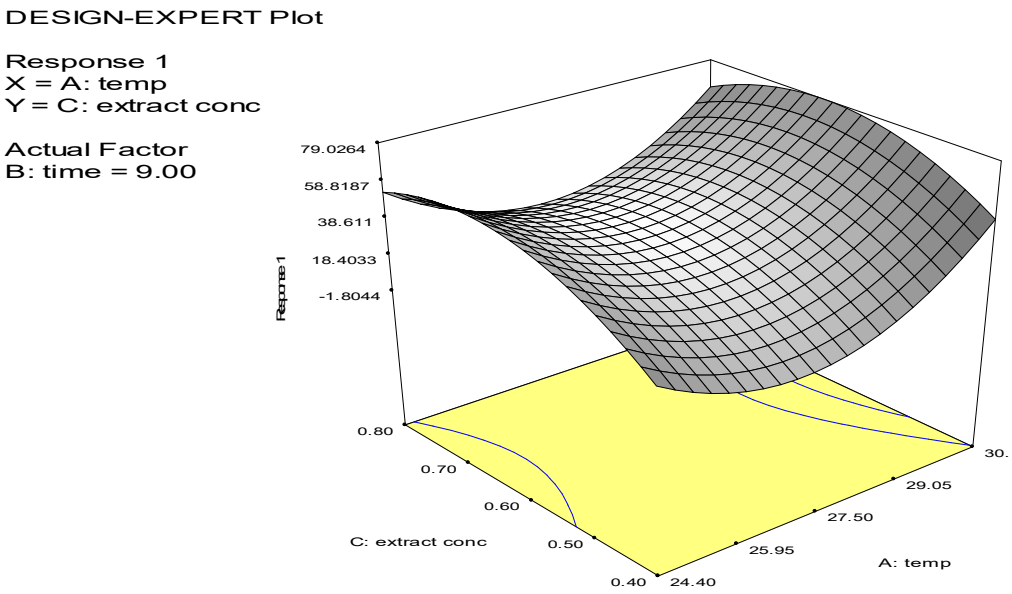

Figure 5: Plot of T *vs.* C of ESE.

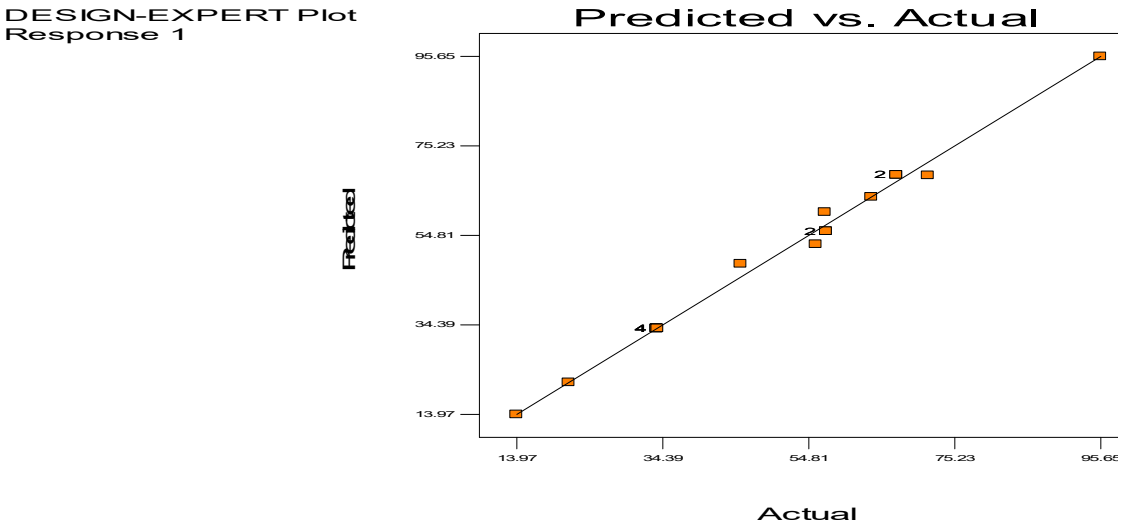

Figure 6: Plot of predicted *vs*. actual values.

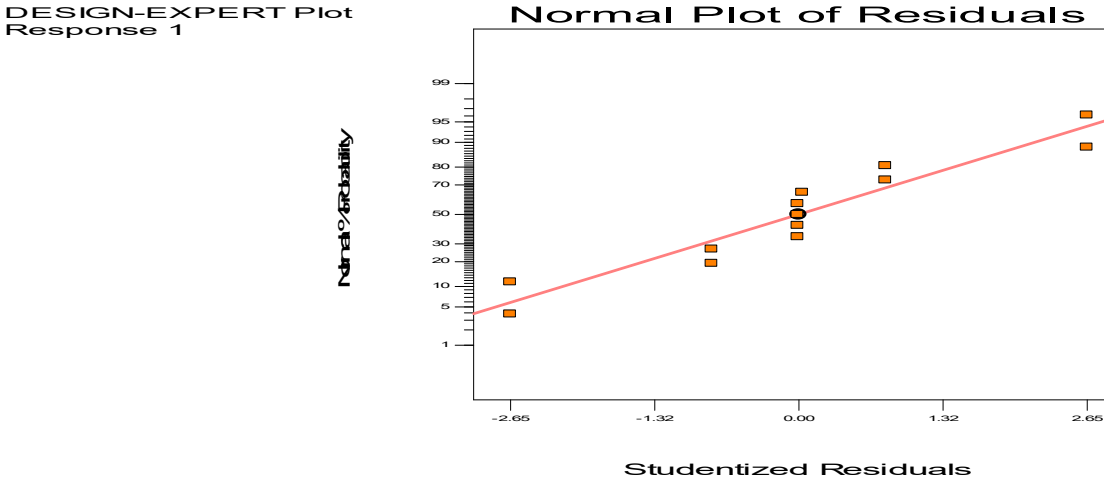

Figure 7: Normal plots residual values vs. Q residuals.

Results of FTIR analysis

Fig. 8 (a-c) shows FTIR spectra of MS immersed in NaCl without inhibitor, with ESE, at its highest IE(%), as a result of the experimental design, and the validated optimal process level, respectively. The bands corresponding to O-H, C-H, O-H, C=N, C-H, O-H and C=C, for MS immersed in NaCl without and with ESE, at its highest IE(%), are 3598.13, 3210.55, 2527.03, 2350.74, 2000.08, 1426.28 and 1096.32 cm^{-1}, respectively. MS immersed in NaCl without inhibitor had a transmittance percentage from 62.71 to 39.26, while with, its highest IT, it was from 48.71 to 26.00. The bands at 3500.26, 3200.41, 3098.15, 2043.15, 2000.08, 1325.80, 1100.73 and 750.26 cm^{-1} were at optimum process level.

The peak at 3500.26 cm^{-1} represents the stretching vibrations of O-H group. 3200.41 cm^{-1} is C-H stretching vibration. 3098.15 cm^{-1} is C-H symmetric stretching vibration of the CH_2 group connection. 2043.15 cm^{-1} is C-N stretching vibration of conjugated ketone or alkene. 2000.80 cm^{-1} is C-N symmetric stretching vibration of the CH_2 group connection. 2043.15 cm^{-1} is C-N stretching vibration amide. ESE functioned as a mixed CI of validated optimal process level, which agreed with findings on CNE by [22, 28].

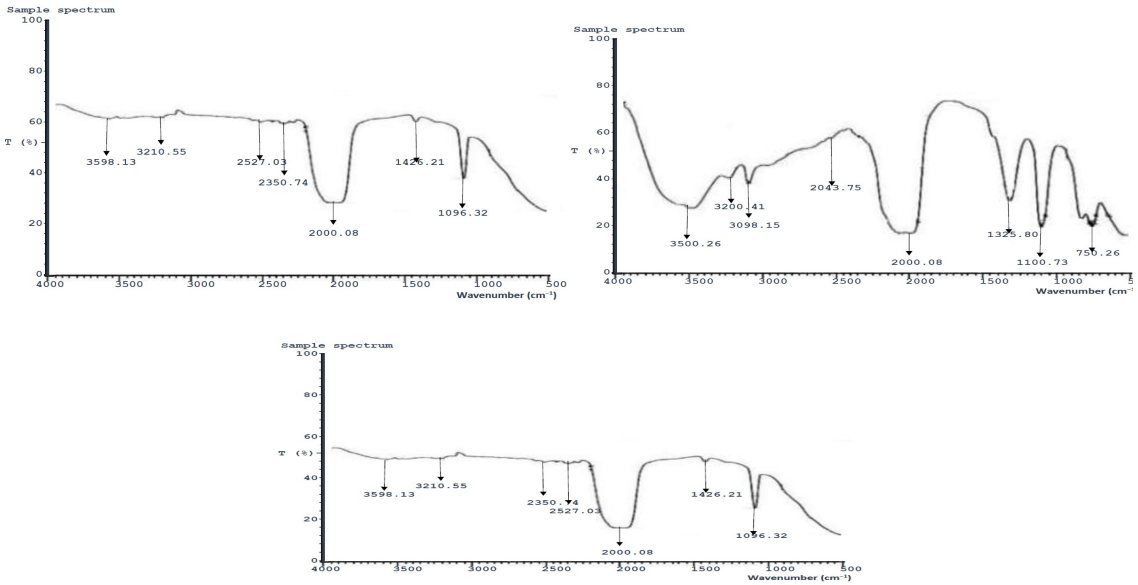

Figure 8: FTIR spectra of MS: **a)** without ESE; **b)** with ESE at its highest IE(%); and **c**) at optimal process level.

Results of SEM analysis

Figs. 9-11 show micrographs of MS immersed in 30 wt% NaCl with and without ESE, respectively.

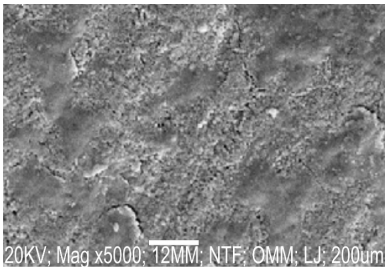

Figure 9: SEM micrographs of MS in 30 wt% NaCl (blank).

The blank coupon was highly corroded with cracks, as shown in Fig. 9. Fig.10, which was derived from experimental design, shows the layers formed by ESE protective film, whereas Fig. 11 (validated optimal level) depicts a more protective film that was due to ESE adsorption [25]. Studies on IE(%) of CNE against MS corrosion in 2 M H_2SO_4 backed up this finding.

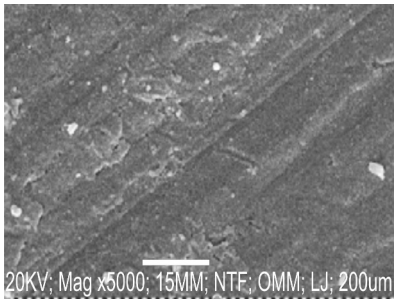

Figure 10: SEM micrographs of MS in 30 wt% NaCl with ESE at its highest IE(%).

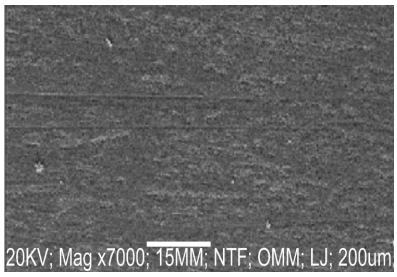

Figure 11: SEM micrographs of MS in 30 wt% NaCl with ESE at its optimal IE(%).

PDP results

Fig. 12 shows the polarization map of MS in 30 wt% NaCl without and with 0.4, 0.6 and 0.8 g/L ESE. ESE worked as a mixed-type CI, as evidenced by E_{corr} displacement (Table 8), which was less than 85 mV [27- 29].

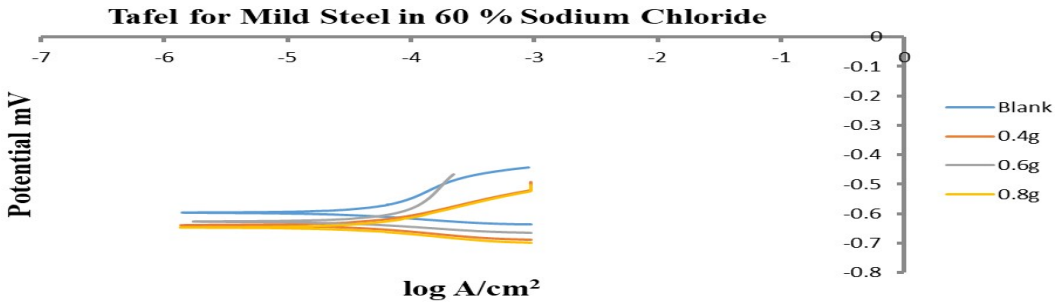

Figure 12: PDP plot.

Table 8: PDP parameters for MS corrosion in 30 wt% NaCl with ESE.

C (g/L)	E_{Corr} (V)	I_{Corr} (A/cm^2)	CR (mm/yr)	R_p (Ω)	β_a (v/dec)	β_c (v/dec)
Blank	-0.59747	0.0000011895	0.013822	442.41	0.0020693	0.0029237
0.4	-0.6394	0.000001086	0.012619	435.49	0.0026357	0.0018557
0.6	-0.62701	0.0000010752	0.012494	426.16	0.0020757	0.0021455
0.8	-0.64813	0.000001007	0.011701	412.08	0.0019249	0.0021929

At 0.4 g/L ESE, CR of MS was the lowest and R_p was the highest, indicating that this C was the most effective. Furthermore, it was also seen that ESE addition blocked MS active sites, which slowed down CR. WL and PDP results were in good agreement.

Results of EDXS analysis

The elemental compositions of MS without and with ESE, at its highest IE(%) and via best process variables, were investigated using EDXS, as shown in Fig. 13 (a-c). Fig. 13c shows O heteroatom larger amount, which could be due to Fe oxidation (Fig 13b). It is manifest that corrosion damage was minimised, as depicted in Fig. 13c, which confirmed the result of [30].

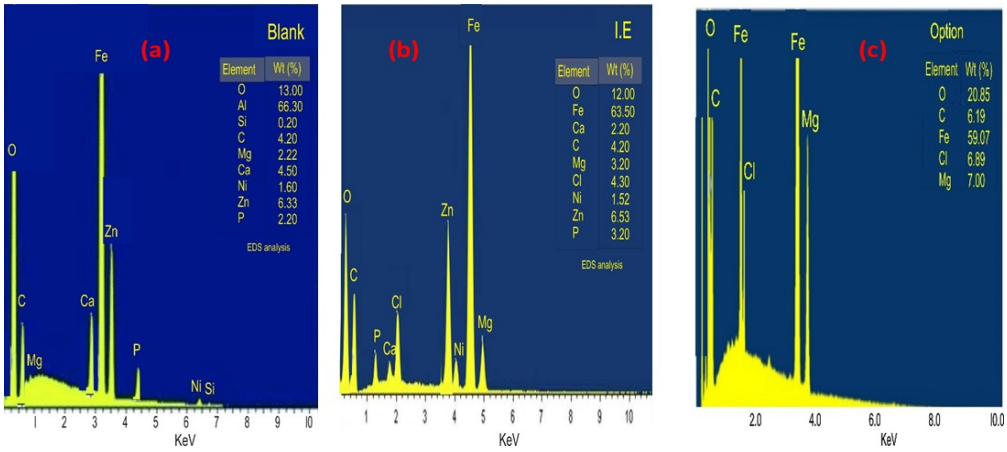

Figure 13: EDXS of MS in 30 wt% NaCl: **(a)** blank; **(b)** with ESE at its highest IE(%); and **(c)** with ESE at its optimal IE(%).

Conclusion

The presence of proteins (a type of amino acid), N, fat and moisture content in the Pc analysis confirmed that ESE is an effective CI. The results of the experimental design showed ESE highest IE(%) of 95.33%, with IT of 6 days, C of 0.4 g/L and T of 24.4 ºC. PDP results showed that the lowest CR was obtained at experiment 4. Results from PDP and WL techniques were in good agreement. SEM outcomes showed that a more passive film was formed on the MS surface, via the optimal process level, than on that with ESE best IE(%). This confirmed that ESE is an effective and environmentally friendly CI.

Acknowledgments

The authors appreciate Landmark University, Omu-Aran, Nigeria, for their support to this research, and provision of facilities.

Authors' contributions

O. Oyewole: wrote the manuscript; interpreted the data; conceived the idea; analyzed the results. **J. B. Adeoye**: wrote the manuscript; interpreted the data; analyzed the results. **M. Lucas**: performed the experiment and interpreted data; analyzed the results; did the experimental design. **W. Olugbemi**: analyzed the results.

Abbreviations

BB: Box-Behnken
C: concentration
CI: corrosion inhibitor/inhibition
CNE: chicken nail extract
CR: corrosion rate
DF: degree of freedom
E_{corr}: corrosion potential
EDXS: energy disperse x-ray spectroscopy
ES: eggshell
ESE: eggshell extract
FTIR: Fourier transform infrared spectroscopy
I_{corr}: corrosion current
IE(%): inhibition efficiency
IT: immersion time
LE: leaves extract
MS: mild steel
NaCl: sodium chloride
OCP: open circuit potential
OPL: optimal process level
Pc: physochemical
PDP: potentiodynamic polarization
Q: studentized range of means divided by the mean estimated standard error for a set of compared samples
R^2: determination coefficient
R_p: polarization resistance
SEM: scanning electron microscopy
SR: scan rate
T: temperature
WL: weight loss

Symbols definition

β_a: Tafel anodic slope
β_a: Tafel cathodic slope
θ: degree of surface coverage

References

1. Feng Z, Hurley B, Li J, Buchheit R. Corrosion inhibition study of aqueous vanadate on Mg alloy AZ31. J Electrochem Soc. 2018;165(2):C94-C102. http://dx.doi.org/10.1149/2.1171802jes
2. Rajalakshmi R, Subhashini S, Leelavathi S et al. Study of the inhibitive action of bakery waste for corrosion of mild steel in acid medium. J Nepal Chem Soc. 2010;25:29-36. 10.3126/jncs.v25i0.3282
3. Omotosho OA, Okeniyi JO, Oni AB, Makinwa TO et al. Inhibition and mechanism of *Terminalia catappa* on mild-steel corrosion in sulphuric-acid environment. Prog Industr Ecolog Int J. 2016;10(4):398-413. https://doi.org/10.1504/PIE.2016.083924

4. Fayomi OS, Akande IG. Corrosion mitigation of aluminium in 3.65% NaCl medium using hexamine. J Bio- Tribo-Corros. 2019;5(1):23. https://doi.org/10.1007/s40735-018-0214-4
5. Rani BE, Basu BB. Green inhibitors for corrosion protection of metals and alloys: An overview. Int J Corros. 2012:1687-9325. https://doi.org/10.1155/2012/380217
6. El-Sayed Shehata O. Effect of acetamide derivative and its Mn-complex as corrosion inhibitor for mild steel in sulphuric acid. Egypt J Chem. 2017;60(2):243-59. https://doi.org/10.21608/ejchem.2017.674.1014
7. Loto CA. The effect of mango bark and leaf extract solution additives on the corrosion inhibition of mild steel in dilute sulphuric acid-Part 1. Corros Prevent Cont. 2001:48(1):38-41.
8. Dehghani A, Bahlakeh G, Ramezanzadeh B. Green Eucalyptus leaf extract: a potent source of bio-active corrosion inhibitors for mild steel. Bioelectrochemistry. 2019;130:107339. https://doi.org/10.1016/j.bioelechem.2019.107339
9. Wang Q, Tan B, Bao H et al. Evaluation of Ficus tikoua leaves extract as an eco-friendly corrosion inhibitor for carbon steel in HCl media. Bioelectrochemistry. 2019;128:49-55. https://doi.org/10.1016/j.bioelechem.2019.03.001
10. Ramezanzadeh M, Bahlakeh G, Ramezanzadeh B. Study of the synergistic effect of Mangifera indica leaves extract and zinc ions on the mild steel corrosion inhibition in simulated seawater: computational and electrochemical studies. J Mol Liq. 2019;292:111387. https://doi.org/10.1016/j.molliq.2019.111387
11. Hussin MH, Kassim MJ, Razali NN et al. The effect of Tinospora crispa extracts as a natural mild steel corrosion inhibitor in 1 M HCl solution. Arab J Chem. 2016;9:S616-24. https://doi.org/10.1016/j.arabjc.2011.07.002
12. Anadebe VC, Onukwuli OD, Omotioma M et al. Optimization and electrochemical study on the control of mild steel corrosion in hydrochloric acid solution with bitter kola leaf extract as inhibitor. S Afr J Chem. 2018;71:51-61. https://doi.org/10.17159/0379-4350/2018/v71a7
13. Baran E, Cakir A, Yazici B. Inhibitory effect of Gentiana olivieri extracts on the corrosion of mild steel in 0.5 M HCl: Electrochemical and phytochemical evaluation. Arab J Chem. 2019;12(8):4303-19. https://doi.org/10.1016/j.arabjc.2016.06.008
14. Eletta OA, Ajayi OA, Ogunleye OO et al. Adsorption of cyanide from aqueous solution using calcinated eggshells: Equilibrium and optimisation studies. J Environ Chem Eng. 2016;4(1):1367-75. https://doi.org/10.1016/j.jece.2016.01.020
15. Dominic OO, Monday O. Optimization of the inhibition efficiency of mango extract as corrosion inhibitor of mild steel in 1.0 M H_2SO_4 using response surface methodology. J Chem Tech Metall. 2016;51(3).
16. Ogunleye OO, Arinkoola AO, Eletta OA et al. Green corrosion inhibition and adsorption characteristics of Luffa cylindrica leaf extract on mild steel in hydrochloric acid environment. Heliyon. 2020;6(1):e03205. https://doi.org/10.1016/j.heliyon.2020.e03205
17. Emori W, Zhang RH, Okafor PC et al. Adsorption and corrosion inhibition performance of multi-phytoconstituents from *Dioscorea septemloba* on carbon steel in acidic media: Characterization, experimental and theoretical studies. Colloi Surf. A: Physicochem Eng Asp. 2020;590:124534. https://doi.org/10.1016/j.colsurfa.2020.124534

18. Ahanotu CC, Onyeachu IB, Solomon MM et al. *Pterocarpus santalinoides* leaves extract as a sustainable and potent inhibitor for low carbon steel in a simulated pickling medium. Sust Chem Pharm. 2020;15:100196. https://doi.org/10.1016/j.scp.2019.100196
19. Salim AM, Dawood NM, Ghazi R. Pomegranate Peel Plant Extract as Potential Corrosion Inhibitor for Mild Carbon Steel in a 1 M HCl Solution. In IOP Conf Series: Mat Sci Eng. 2020;987(1),12019. https://doi.org/10.1088/1757-899X/987/1/012019
20. Hossain N, Chowdhury MA, Iqbal AP et al. Paederia foetida leaves extract as a green corrosion inhibitor for mild steel in hydrochloric acid solution. Curr Res Green Sust Chem. 2021;4:100191. https://doi.org/10.1016/j.crgsc.2021.100191
21. Olawale O, Ogunsemi BT, Abayomi SJ et al. Optimization of *Katemfe* Seed Extract as a Corrosion Inhibitor for Mild-Steel in 0.5 M HCl. Int J Civil Eng Tech. 2018;9(13):1394-402.
22. Olawale O, Bello JO, Ogunsemi BT et al. Optimization of chicken nail extracts as corrosion inhibitor on mild steel in 2 M H_2SO_4. Heliyon. 2019;5(11):e02821. https://doi.org/10.1016/j.heliyon.2019.e02821
23. Oyewole O, Oshin TA, Atotuoma BO. *Corchorus olitorius stem* as corrosion inhibitor on mild steel in sulphuric acid. Heliyon. 2021;7(4):e06840. https://doi.org/10.1016/j.heliyon.2021.e06840
24. Oyewole O, Aondoakaa E, Abayomi TS et al. Characterization and optimization study of *Ficus exasperata* extract as corrosion inhibitor for mild steel in seawater. World Sci News. 2021;51:78-94.
25. Ogunleye OO, Eletta OA, Arinkoola AO et al. Gravimetric and quantitative surface morphological studies of *Mangifera indica* peel extract as a corrosion inhibitor for mild steel in 1 M HCl solution. Asia-Pac J Chem Eng. 2018;13(6):e2257. https://doi.org/10.1002/apj.2257
26. Ibrahim M, Kannan K, Parangusan H et al. Enhanced corrosion protection of epoxy/ZnO-NiO nanocomposite coatings on steel. Coatings. 2020;10(8):783. https://doi.org/10.3390/coatings10080783
27. Sanni O, Popoola AP, Fayomi OS. The inhibitive study of egg shell powder on uns n08904 austenitic stainless-steel corrosion in chloride solution. Def Tech. 2018;14(5):463-8. https://doi.org/10.1016/j.dt.2018.07.015
28. Hu J, Chen H, Dong H et al. Transformation of iopamidol and atrazine by peroxymonosulfate under catalysis of a composite iron corrosion product (Fe/Fe3O4): Electron transfer, active species and reaction pathways. J Haz Mater. 2021,5;403:123553. https://doi.org/10.1016/j.jhazmat.2020.123553
29. Kumar CP, Mohana KN. Phytochemical screening and corrosion inhibitive behavior of *Pterolobium hexapetalum* and *Celosia argentea* plant extracts on mild steel in industrial water medium. Egy J Pet. 2014;23(2):201-11. https://doi.org/10.1016/j.ejpe.2014,05.007
30. Alrefaee SH, Rhee KY, Verma C et al. Challenges and advantages of using plant extract as inhibitors in modern corrosion inhibition systems: Recent advancements. J Mol Liq. 2021;(1)321:114666. https://doi.org/10.1016/j.molliq.2020.114666